JOURNAL OF MAGNETIC RESONANCE 97, 398–410 (1992)

Simulating the Effect of the Two-Spin Approximation on the Generation of Protein Structures from NOE Data

DOROTHEA KOMINOS,* ASIF K. SURI, DOUGLAS B. KITCHEN, DONNA BASSOLINO,† AND RONALD M. LEVY‡

Department of Chemistry, Rutgers University, P.O. Box 939, Piscataway, New Jersey 08855-0939

Received July 1, 1991; revised October 1, 1991

The use of structural information derived from NMR data, when combined with computer modeling techniques, has enabled the structures of many proteins to be determined (*1–6*). Among the most useful structural information is interproton distances which can be derived from nuclear Overhauser enhancement experiments. For small rigid molecules, the intensity of the NOE between protons i and j is proportional to the inverse sixth power of the distance between the two protons. In macromolecules, indirect magnetization transfer (spin diffusion) from nearby protons and intramolecular dynamics affect the magnitude of the NOE between protons i and j and contribute to errors in estimating interproton distances from NOE cross peaks (*7–9*). Several methods have been proposed for dealing with the spin-diffusion problem. These methods make use of the relaxation matrix to incorporate multispin effects (*10–14*). The simplest but least systematic approach is to calculate a theoretical spectrum from the relaxation matrix using a trial structure, and to adjust distances by trial and error between pairs of protons whose calculated cross peaks have the largest deviations from the experimental values (*15–18*). In another approach theoretical cross peaks from a trial structure are merged with experimental NOEs (*12, 19, 20*), and after the solution of the Bloch equations is inverted to obtain the relaxation matrix, the resulting distances can be added as constraints in a molecular-dynamics or distance geometry refinement. The most rigorous and computationally intensive procedures involve the direct refinement of calculated against experimental NOE spectra, either by analytically evaluating the gradients of the calculated NOEs with respect to coordinates (*21–23*) or by using a Monte-Carlo procedure (*24*). Despite the recent focus on incorporating spin-diffusion effects in the refinement of macromolecular structures, it is unclear how much error is introduced by spin diffusion. This is of interest because, although the direct refinement of calculated against experimental NOE intensities is in principle the more "correct" procedure, it is much more computationally intensive than re-

* Present address: The Rockefeller University, New York, New York 10021.

† Present address: Bristol-Myers Squibb Pharmaceutical Research Institute, P.O. Box 4000, Princeton, New Jersey 08543-4000.

‡ To whom correspondence should be addressed.

0022-2364/92 $3.00

finement against estimated distances based on the two-spin approximation which ignores spin diffusion. Furthermore, there are additional problems encountered when refining directly against spectra, e.g., how to treat experimental noise (*14*). Also, for at least a few cases, protein structures derived from NMR data using the two-spin approximation have been shown to be close to the corresponding crystal structures, and this suggests that in some circumstances spin-diffusion effects are unimportant (*25–27*). The generation and refinement of a protein structure starting with NOE data and a modeling procedure is a highly nonlinear problem with very many variables which affect the quality of the final structure. In this Communication we use simulations to demonstrate how the number of constraints and the refinement procedure can influence the structural errors induced by spin diffusion.

To explore the effects of the two-spin approximation on protein structures, we have exploited a modeling strategy which has been previously employed in an analogous manner to analyze the relationship between temperature factors and atomic mobility in macromolecular crystallographic refinement (*28, 29*). Starting with the coordinates from a known protein structure we generate an "ideal" experimental data set—for the NMR experiment this corresponds to calculating NOE intensities by solving the relaxation matrix equations. We can then treat these intensities as if they were experimental data (from which the noise had been removed). We then make the two-spin approximation and extract interproton distances from the simulated intensity data set. These "two-spin distances" are then used as input in a protein structure generation and refinement program. In this Communication we focus on two results from this modeling: (1) the systematic errors in the estimates of interproton distances introduced by the two-spin approximation which arise from the geometric relationships of the proton spins in a protein, and (2) the effects of these errors on generated structures using one particular refinement protocol. As we were writing up this work, a closely related study was published (*30*) and we comment on the similarities and differences between the two studies.

We have chosen to use the protein Crambin as the model system. All the calculations were carried out with the IMPACT program package (*31–33*). Protons were added to the heavy atom coordinates (*34*) obtained from the Brookhaven protein data bank and the structure was energy-minimized. This target structure contained 1221 interproton distances less than 5 Å which could potentially give rise to observable NOEs. However, for a variety of reasons for proteins it is very common to be able to quantitate far fewer than the theoretical maximum number of observable NOEs. As discussed below and analyzed in detail elsewhere, the number of NOEs used in the refinement affects our conclusions regarding the errors in protein structures introduced by the use of the two-spin approximation. For the analysis presented here we have carried out simulations with two different constraint sets. In the first, corresponding to an "intermediate quality" data set, we have selected 50% of the 1221 proton pairs for structure generation and refinement; these pairs were selected at random. To these target distances, error bounds were added as described below. In the second set of simulations, corresponding to a "high quality" data set, all 1221 distance constraints were used in the structure generation and refinement.

The evolution of the NOE intensities as a function of mixing time t_m is described by the Bloch equations (*35*),

$$\frac{d}{dt}\mathbf{N}(t) = -\sigma\mathbf{N}(t), \qquad [1]$$

where **N** is the matrix of cross-peak intensities. The elements of the relaxation matrix σ contain the structural information

$$\sigma_{ij} = \frac{\gamma^4 h^2}{10\langle r_{ij}^3\rangle 2}\,[6J(2\omega) - J(0)] \qquad [2a]$$

$$\sigma_{ii} = E_i + \sum_{j\neq i} \sigma_{ij} \qquad [2b]$$

$$J(\omega) = \frac{\tau_c}{1 + \omega^2\tau_c^2}, \qquad [2c]$$

where ω and γ are the resonance frequency and the gyromagnetic ratio for ^{1}H nuclei, respectively, and E_i is the external relaxation rate of spin i. E_i was constant for all spins with a value of 0.5 sec^{-1}. For the spectral density function, $J(\omega)$, we assume an isotropic tumbling model with relaxation time τ_c. Given a structural and motional model from which the elements of the relaxation matrix are constructed, the Bloch equation can be integrated analytically to obtain the cross-peak intensities at mixing time t_m,

$$\mathbf{N}(t_m) = \mathbf{U}^t\mathbf{e}^{-\lambda t}\mathbf{U}\mathbf{N}(0), \qquad [3]$$

where $\mathbf{e}^{-\lambda t}$ is a diagonal matrix, λ is an eigenvalue of σ, and **U** is the matrix of eigenvectors. Of course the elements $N_{ij}(t_m)$ depend on the geometric relation of protons i and j to all the other protons and not just the distance between protons i and j. However, in the linear two-spin approximation and in the absence of internal motion, the following relation is used to estimate r_{ij} from a measured (or simulated) cross-peak intensity $N_{ij}(t_m)$,

$$\frac{N_{ij}(t_m)}{N_{kl}(t_m)} = \frac{\sigma_{ij}}{\sigma_{kl}} = \frac{r_{kl}^6}{r_{ij}^6}, \qquad [4]$$

where N_{kl} and r_{kl} correspond to the intensity and distance of a calibrating proton pair; e.g., a common choice is the NOE between two methylene protons.

In Figs. 1a and 1b are shown scatter diagrams of the actual interproton distances for each of the 1221 protons measured from the Crambin crystal structure versus the distances estimated from the simulated NOE data using Eq. [4]. The NOE data were simulated with the following parameters: ω = 500 MHz, τ_c = 5 ns, and two different mixing times t_m = 150 ms (Fig. 1a) and t_m = 400 ms (Fig. 1b). As pointed out previously by Post *et al.* (*14*), who performed similar calculations, and by Borgias and James (*12*), spin-diffusion effects introduce systematic errors in the apparent distances, with longer distances appearing to be shorter than they actually are. For protons i and j which are far apart there is a greater probability that there will be intervening protons which can effectively relay the NOE from i through k to j than for proton pairs which are closer together. This leads to a larger NOE and an apparently shorter distance r_{ij} when the two-spin approximation is employed. Also there are some interproton distances which appear to be longer than they actually are. As is clear from Fig. 1, the effects are accentuated at the very long mixing time, but the errors are quite substantial even at 150 ms. The distributions of the errors in the distances

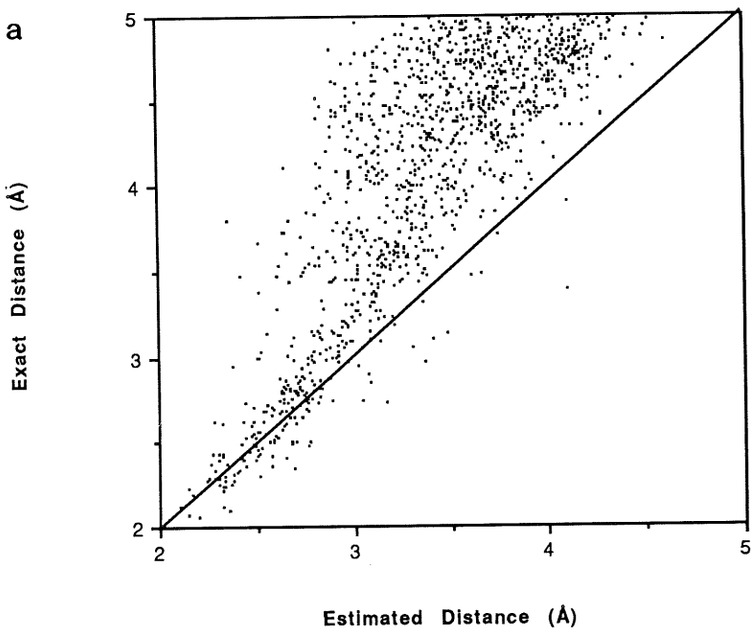

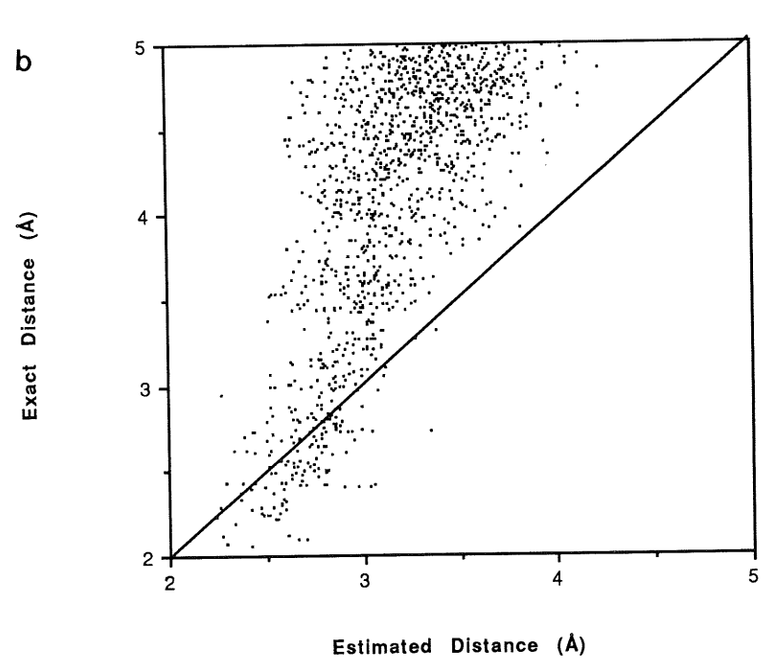

FIG. 1. The exact interproton distance is plotted against the distance estimated from the simulated NOE data set using the linear two-spin approximation. NOEs simulated using a mixing time (a) t_m = 150 ms and (b) t_m = 400 ms.

are plotted in Figs. 2a and 2b. With a 150 ms mixing time, 1140 of the 1221 distances are calculated from the two-spin approximation to be smaller than the true distances. The average decrease is 0.75 Å from the actual target distance; the maximum decrease is 2.4 Å. Similar results are obtained for the 400 ms data set, but the average error (decrease in the distance) is 1.02 Å, and the largest error is 2.1 Å for this data set. We turn now to the question of how these errors in the interproton distances, which are caused by the application of the two-spin approximation to the simulated NOE data set, affect the structures generated from these distances.

In order to generate Crambin structures from the different sets of distances, we used an internal-coordinate Monte-Carlo algorithm coupled to a molecular-dynamics refinement described previously (*31–33*). The refinement consists of optimizing a target function which is a sum of molecular-mechanics terms (*36*) plus a term which contains the distance constraints. The distance constraints are implemented in the form of constraint ranges. That is, the target interproton distances are assigned to categories (corresponding to strong, medium, and weak NOEs) and the constraints are said to be satisfied if the target distance falls within a certain range. This is a commonly used device whose rationale is that the use of constraint ranges accounts for various sources of error in the estimates of interproton distances from NOEs (*1–6, 25*). Furthermore, it is assumed that distances estimated from stronger NOEs can be estimated with greater accuracy than those estimated from weaker ones. There has been some analysis of the effects of these constraints on refined structures (*37, 38*). The constraint ranges which we have employed, corresponding to strong, medium, and weak NOEs, are:

Strong:	$d < 3.0$ Å	$d_{\text{lower}} = d - 0.5$ Å	$d_{\text{upper}} = d + 0.5$ Å
Medium:	$3.0 \text{ Å} \leqslant d < 4.0$ Å	$d_{\text{lower}} = d - 0.5$ Å	$d_{\text{upper}} = d + 1.0$ Å
Weak:	$4.0 \text{ Å} \leqslant d < 5.0$	$d_{\text{lower}} = d - 1.0$ Å	$d_{\text{upper}} = d + 1.0$ Å

With these constraint ranges, we use a biharmonic form of the constraining potential in the target function if the calculated distance falls outside the constraint range; when the distance is within the constraint range the potential is set to zero. Note that the constraint ranges get tighter as the target distances decrease. Thus as a consequence of the systematic decrease in target distances caused by the use of the two-spin approximation, there is also a systematic tightening of the constraint ranges. Thus, in the simulated data constructed with a 150 ms mixing time, 717 of the 1221 constraints are shifted to a tighter constraint range. The number of constraints is summarized in Table 1.

The results of the structure generation and refinement using the different interproton distance data sets are shown in Table 2. The rms backbone deviation between the seven converged structures obtained using the exact distances (with their associated ranges) as the target was 1.42 ± 0.21 Å rms deviation from the Crambin crystal structure. Surprisingly, the rms deviations from the crystal structure of those structures refined using the simulated two-spin distances (with their associated ranges) as targets are smaller than those generated using the exact distances. The average rms deviation is 0.78 ± 0.40 Å from the crystal structure when the distances from the 150 ms data set are used as targets and 0.96 ± 0.41 when the distances from the 400 ms data set are used. These results are counterintuitive. How can the use of target distances which contain systematic errors due to spin diffusion lead to structures which more closely

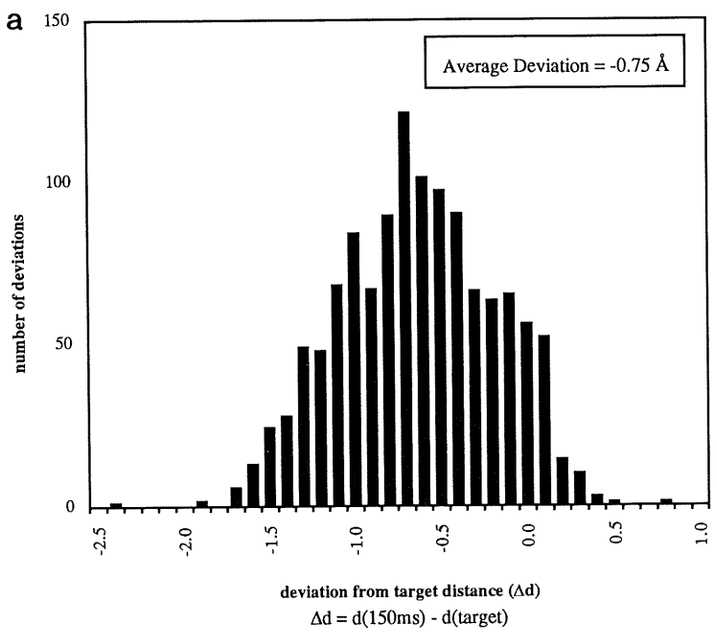

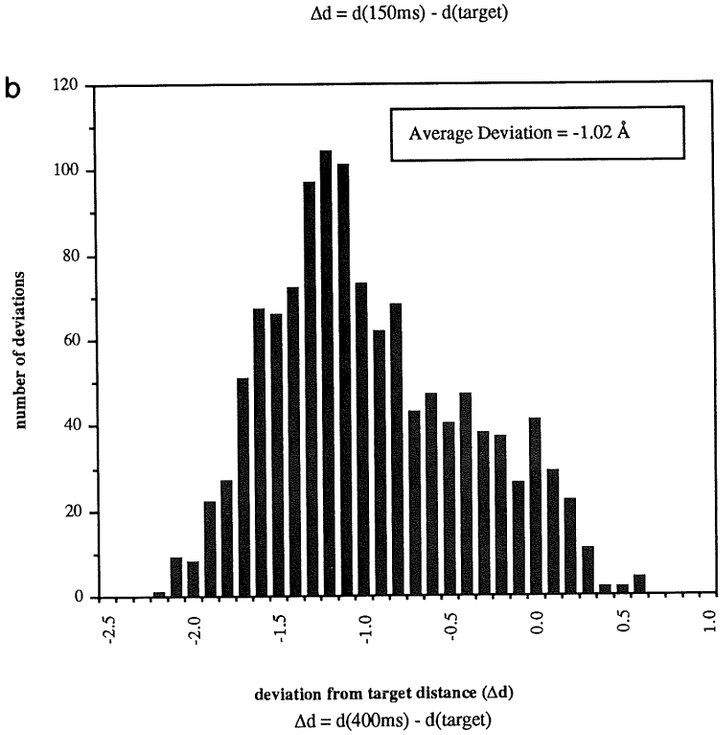

FIG. 2. (a) Distributions of differences between the simulated distances derived using the two-spin approximation assuming a 150 ms mixing time and the exact distances measured directly from the Crambin crystal structure. (b) Same as (a) except 400 ms mixing time.

TABLE 1

Number of Constraints in Each Constraint Range

Set	Type of constraints	Number of constraints		
		Short[a]	Medium[b]	Long[c]
DIST	Exact distances	68	144	398
TSA	Two-spin distances 150 ms mixing time	142	379	89
TSB	Two-spin distances 400 ms mixing time	226	380	4

[a] Distances less than 3.0 Å.
[b] Distances between 3.0 and 4.0 Å.
[c] Distances between 4.0 and 5.0 Å.

resemble the crystal structure than the use of exact target distances? As discussed below, the number of distance constraints and the constraint ranges used in the simulations both affect the relative error introduced by the use of "two-spin distances" as targets in the refinement.

Considering first the structures generated using exact interproton distances as the target, the largest number of distances (398 out of 610) falls in the loose constraint range (i.e., they correspond to weak NOEs). Within this group, the deviations from the target distances show a broad distribution (Fig. 3a) with the average value somewhat larger than the target distance. In contrast, for the two-spin data set constructed with a 150 ms mixing time, the largest number of distances (379 out of 610) falls in the medium constraint range. Within this group, the deviations from the target distances are more narrowly distributed (as expected from the application of tighter constraints) but are also more sharply peaked about a positive deviation from the target distance of about 1 Å (Fig. 3b). Therefore, while the target distances for this data set are on the average 0.75 Å too small because of spin-diffusion effects, the distances in the refined structures are approximately 1 Å larger than the target values and by this cancellation of errors, they end up close to the exact distances. A schematic diagram summarizing the relationship between constraint ranges and distance distributions is shown in Fig. 4. Similar results are obtained for the spin-diffusion data set constructed with a 400 ms mixing time. This suggests that it should be possible to generate reasonably accurate protein structures using the two-spin approximation from NOE data sets collected at long mixing times where the signal-to-noise is high, even though spin diffusion causes significant errors in the target distances. Further work is needed to delineate the appropriate conditions for employing such a procedure.

As stated above, solving a protein structure from NOE data is a highly nonlinear problem. It is difficult to anticipate the ways in which all the variables can interact to affect the quality of the final structure. One variable we have studied is the percentage of total constraints used in the refinement. Our simulations suggest that, in contrast to the results presented above, when very high quality data are available, the use of the two-spin approximation does indeed result in less accurate structures as expected. Our "high quality" data set consisted of all 1221 distance constraints for Crambin. In

TABLE 2

Average rms Deviations for Structures Generated Using Constraints Measured Directly from the Target Structure and Those Using Distances Derived from the Two-Spin Approximation

50% (610 constraints) of distances with ranges

Set	rms_{bb} (Å)[a]	rms_{aa} (Å)[b]
DIST[c]	1.42 ± 0.21	1.75 ± 0.15
TSA[d]	0.78 ± 0.40	1.20 ± 0.39
TSB[e]	0.96 ± 0.41	1.33 ± 0.43

100% (1221 constraints) of distances without ranges

Set	rms_{bb} (Å)[a]	rms_{bb} (Å)[b]
EXACT[f]	0.20 ± 0.11	0.38 ± 0.16
TSC[g]	0.81 ± 0.12	1.02 ± 0.21
TSD[h]	1.34 ± 0.13	1.61 ± 0.16

Note. The refinements of structures generated using 610 distance constraints were carried out using (strong, medium, and weak) constraint ranges as described in the text. For the refinements of the structures generated with 1221 distance constraints, a harmonic penalty function from the target distance was used without adding a constraint range.

[a] Average backbone rms deviation between the structure generated from distance constraints and the coordinates of the Crambin crystal structure.

[b] Average rms deviation as above including all atoms (including protons).

[c] Set DIST uses (610) constraint distances measured directly from the crystal structure.

[d] Set TSA uses (610) distance constraints estimated from simulated NOE intensities assuming a 150 ms mixing time and using the linear two-spin approximation (Eq. [4]).

[e] Set TSB uses (610) distance constraints estimated from simulated NOE intensities assuming a 400 ms mixing time and using the linear two-spin approximation (Eq. [4]).

[f] Set EXACT uses (1221) distance constraints measured directly from the crystal structure.

[g] Set TSC uses (1221) distance constraints estimated from simulated NOE intensities assuming a 150 ms mixing time and using the linear two-spin approximation (Eq. [4]).

[h] Set TSD uses (1221) distance constraints estimated from simulated NOE intensities assuming a 400 ms mixing time and using the linear two-spin approximation (Eq. [4]).

these simulations the refinement was carried out using a harmonic penalty function from the target distance without adding an additional constraint range. The results of our simulations with this data set are listed in Table 2. When exact distances were

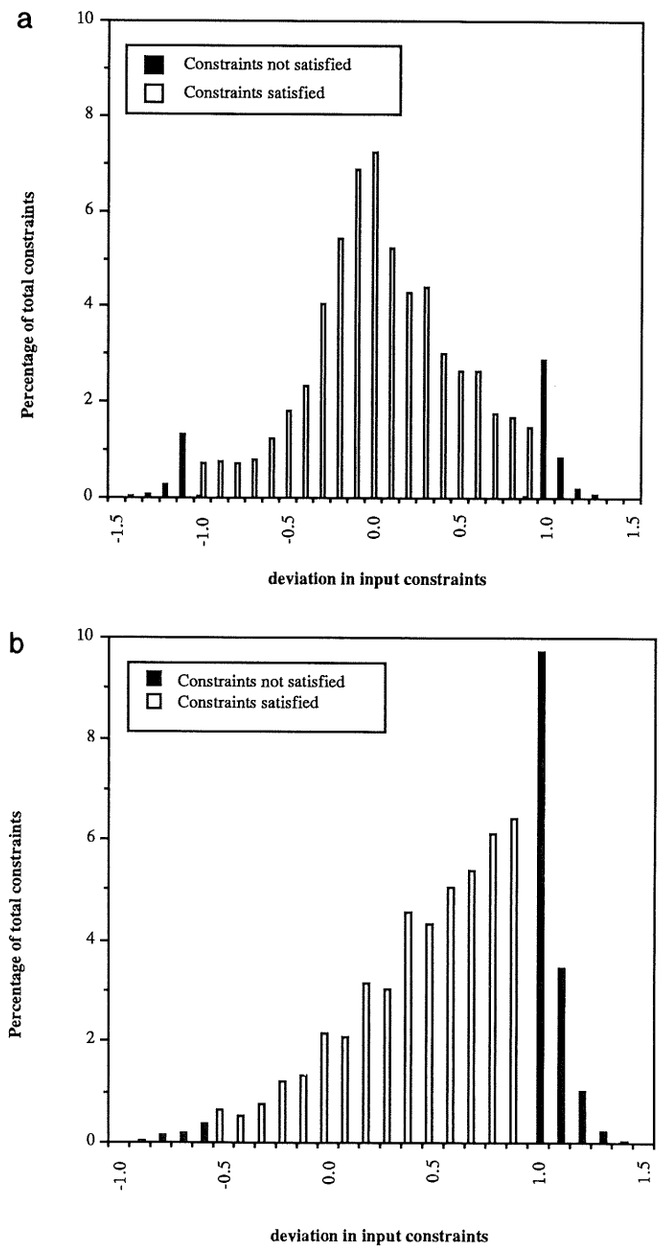

FIG. 3. Distribution of deviations between the input constraint distances and the corresponding distances in the refined Crambin structures generated from the distance constraints. (a) Distribution of the deviations in the long range (4 Å $\leq r_{ij} <$ 5 Å) constraints; these structures were generated using constraints derived from the exact interproton distances calculated from the crystal structure (set DIST). (b) Distribution of the deviations in the medium range (3 Å $\leq r_{ij} <$ 4 Å) constraints; these structures were generated from distances estimated from the simulated NOE data set using the linear two-spin approximation with a 150 ms mixing time (set TSA).

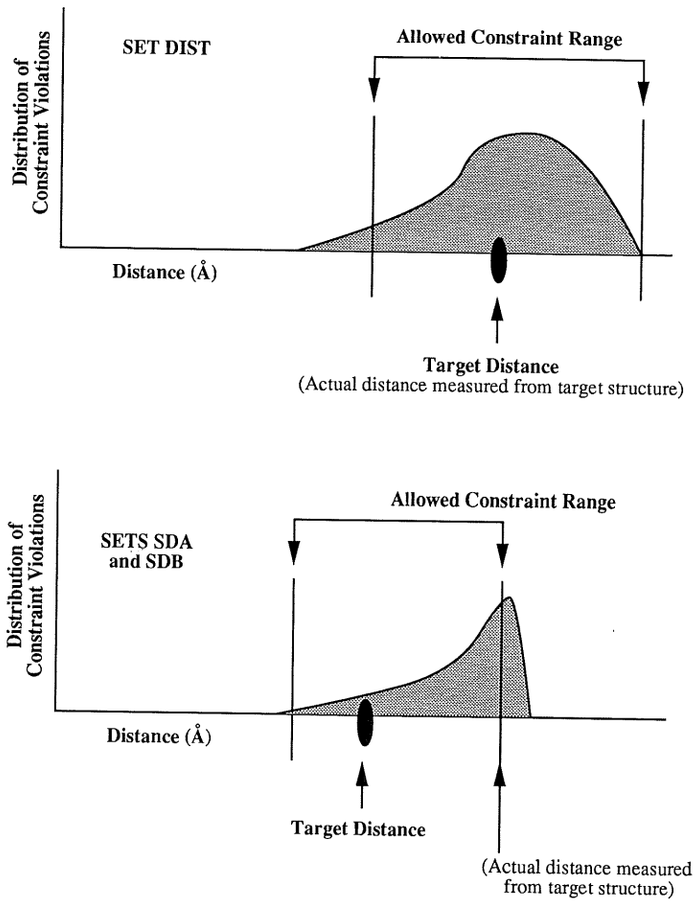

FIG. 4. Schematic diagram illustrating the shape of the distribution of constraint violations in the refined coordinates for the Crambin structures generated using distance constraints based on exact interproton distances (top), and distance constraints estimated from the simulated NOE data set using the linear two-spin approximation (bottom).

used as targets, the rms superposition of the final structures generated from initial random conformations onto the Crambin crystal structure was 0.2 Å. In contrast, when distances extracted from an NOE data set constructed with a 150 ms mixing time to which the two-spin approximation was applied were used as targets, the rms deviation from the crystal structure increased to 0.8 Å. Using the "two-spin distances" extracted from the 400 ms mixing time NOE data as targets, the rms deviation of the refined structures from the crystal structure increased still further to 1.34 Å.

James and co-workers (*30*) have recently reported the results of simulations of spin-diffusion effects at short mixing times on pancreatic trypsin inhibitor (PTI) solution structures. They carried out four sets of simulations. The first uses distances extracted from a relaxation matrix analysis—this set approximates exact distances. The second and third sets of simulations use "two-spin distances" estimated from simulated in-

tensities at a mixing time of 100 ms. To these "two-spin" target distances conservative constraint ranges were added in one set of simulations, and restrictive constraint ranges were added in another set of simulations. A control simulation using exact distances as targets was also completed. The effect of varying the number of constaints was not considered; all the simulations were carried out using 708 distance constraints. The structures were generated from the structural constraints by the distance geometry method. They obtained the best results when the "exact" distances, extracted from the relaxation matrix analysis, were used as targets. These structures had a backbone rms deviation of 1.08 ± 0.10 Å from the crystal structure. When "two-spin distances" were used in conjunction with restrictive constraint ranges, the rms deviation of backbone atoms increased to 1.19 ± 0.09 Å, while when conservative constraint ranges were used, the rms deviation increased further to 1.27 ± 0.11 Å. Since even at short mixing times the use of a two-spin approximation results in systematic errors of 45–80% in distances over 3.5 Å (*30*), it is not obvious that tighter constraint ranges will improve the structures when the two-spin approximation is used. Thomas *et al.* (*30*) conclude from their simulations that as long as the smaller distance ranges are in reasonable agreement with the true distances, more restrictive distance constraints yield more accurate structures even with the "two-spin" approximation.

The analysis of the effect of error bounds in the PTI simulations is consistent with the Crambin simulations. Considering the Crambin simulations using the 50% data set, the shift to tighter constraint ranges when the two-spin approximation was applied improved the accuracy of the structures. The tightening of the constraint ranges was not done artificially to improve the results obtained with the two-spin approximation. Rather, according to the refinement protocol, the constraint range used for NOEs with larger intensities is tighter than the range used with weaker NOEs. Since spin diffusion increases the intensity of NOEs between protons at larger separations, not only are the target distances systematically shortened, but tighter constraints are applied as well. Undoubtedly, the use of tighter constraint ranges would also improve the accuracy of structures refined using the exact distances as targets. It is clear from the simulations of spin-diffusion effects on the refinement of PTI (*30*) and Crambin that both the number of constraints and the constraint ranges used in the refinement affect the magnitude of the errors introduced by the use of the two-spin approximation. The development of constraint-range protocols in protein solution structure refinement has occurred in an ad hoc fashion, with the current trend favoring conservative (loose) constraints. The results of the simulations of spin-diffusion effects on the solution structures of PTI and Crambin suggest that tighter constraints can improve the accuracy of the refined structures even when the two-spin approximation is applied. In view of the large effect that different constraint protocols have on protein refinement, more analysis is needed to optimize refinement strategies.

Summarizing our conclusions regarding the relationship between the number of constraints and the errors introduced by the two-spin approximation, we found that with a complete data set (100% of the total possible constraints used in the refinement, which would be difficult to realize in practice), the application of the two-spin approximation degrades the accuracy of the refined structures to some extent. With an intermediate data set (50% of the total possible constraints used in the refinement), we found that the use of "two-spin distances" actually leads to somewhat better structures with our particular refinement protocol. While the quantitative details will be

sensitive to the particular refinement protocol used, our simulations show in a qualitative sense that the two-spin approximation can be used to generate reasonably accurate structures even at long mixing times (e.g., τ_m = 400 ms). This observation can be used to advantage when refining proteins with NOE spectra exhibiting poor signal-to-noise at short mixing times.

Simulations play an important role in the development of methods for generating and refining macromolecular structures from NMR data. With the exception of the work reported here and the recent work of James and co-workers (*30*), all the simulations we are aware of refined against distances calculated directly from a target structure. Two aspects of the refinement procedure which are often reported are the residual violations of the constraints and the number of structures which converge starting from random initial structures. In the Crambin simulations, we found that when we used the "two-spin distances" as target distances instead of "exact" distances taken from the crystal structure, we had a much lower convergence rate (20% of the initial structures converged) than when exact distances were used (convergence rate of ~50%). This may be related to the fact that the "two-spin distances," which contain spin-diffusion effects, are not self-consistent; that is, they do not correspond to a real structure. Second, we observed that the average residual violations of the NOE distance constraints in the structures generated using the two-spin approximation are considerably larger than those generated from the exact distances. This is not surprising in view of the fact that the coordinates of these structures are "close" to the coordinates of the crystal structure, while the target distances are systematically too short. However, this also implies that the residual distance constraint violations cannot be reduced to zero when using target distances which include substantial spin-diffusion effects. A more complete analysis of these effects will be given elsewhere.

ACKNOWLEDGMENTS

This work has been supported in part by NIH Grant GM-30580. We acknowledge grants of supercomputer time from the National Cancer Institute of the National Institutes of Health and the Pittsburgh Supercomputer Center.

REFERENCES

1. K. WÜTHRICH, "NMR of Proteins and Nucleic Acids," Wiley, New York, 1986.
2. K. WÜTHRICH, *Acc. Chem. Res.* **22,** 36 (1989).
3. A. BAX, *Annu. Rev. Biochem.* **58,** 223 (1989).
4. G. M. CLORE AND A. M. GRONEBORN, *Crit. Rev. Biochem. Mol. Biol.* **24,** 479 (1989).
5. J. L. MARKLEY, *in* "Methods in Enzymology" (N. J. Oppenheimer and T. L. James, Eds.), Vol. 176, p. 12, Academic Press, San Diego, 1989.
6. A. BRUNGER AND M. KARPLUS, *Acc. Chem. Res.* **24,** 54 (1991).
7. A. KALK AND H. J. C. BERENDSEN, *J. Magn. Reson.* **24,** 343 (1976).
8. E. T. OLEJNICZAK, M. KARPLUS, C. M. DOBSON, AND R. M. LEVY, *J. Am. Chem. Soc.* **106,** 1923 (1984).
9. A. N. LANE, *J. Magn. Reson.* **78,** 425 (1988).
10. J. W. KEEPERS AND T. L. JAMES, *J. Magn. Reson.* **57,** 404 (1984).
11. E. T. OLEJNICZAK, R. T. GAMPE, AND S. W. FESIK, *J. Magn. Reson.* **67,** 28 (1986).
12. B. A. BORGIAS AND T. L. JAMES, *J. Magn. Reson.* **79,** 493 (1988).
13. G. M. CLORE AND A. M. GRONENBORN, *J. Magn. Reson.* **84,** 398 (1989).
14. C. B. POST, R. P. MEADOWS, AND D. G. GORENSTEIN, *J. Am. Chem. Soc.* **112,** 6796 (1990).
15. D. MARION, M. GENEST, AND M. PTAK, *Biophys. Chem.* **28,** 235 (1987).
16. J.-F. LEFÈVRE, A. N. LANE, AND O. JARDETZKY, *Biochemistry* **26,** 5076 (1987).

17. W. J. METZLER, C. WANG, D. B. KITCHEN, R. M. LEVY, AND A. PARDI, *J. Mol. Biol.* **214,** 711 (1990).
18. K. M. BANKS, D. R. HARE, AND B. R. REID, *Biochemistry* **28,** 6996 (1989).
19. R. BOELENS, T. M. G. KONING, AND R. KAPTEIN, *J. Mol. Struct.* **173,** 299 (1988).
20. R. BOELENS, T. M. G. KONING, G. A. VAN DER MAREL, J. H. VAN BOOM, AND R. KAPTEIN, *J. Magn. Reson.* **82,** 290 (1989).
21. P. YIP AND D. A. CASE, *J. Magn. Reson.* **83,** 643 (1989).
22. J. D. BALEJA, J. MOULT, AND B. D. SYKES, *J. Magn. Reson.* **87,** 375 (1990).
23. J. D. BALEJA, R. T. PON, AND B. D. SYKES, *Biochemistry* **29,** 4828 (1990).
24. A. K. SURI AND R. M. LEVY, unpublished.
25. G. WAGNER, W. BRAUN, T. F. HAVEL, T. SCHAUMANN, N. GO, AND K. WÜTHRICH, *J. Mol. Biol.* **196,** 611 (1987).
26. M. BILLETER, A. D. KLINE, W. BRAUN, R. HUBER, AND K. WÜTHRICH, *J. Mol. Biol.* **206,** 677 (1989).
27. H. J. DYSON, M. RANCE, R. A. HOUGHTEN, P. E. WRIGHT, AND R. A. LERNER, *J. Mol. Biol.* **201,** 201 (1988).
28. J. G. KURIYAN, G. PETSKO, R. M. LEVY, AND M. KARPLUS, *J. Mol. Biol.* **190,** 227 (1986).
29. E. WESTHOF, B. CHEVRIER, S. GALLION, P. WEINER, AND R. M. LEVY, *J. Mol. Biol.* **190,** 699 (1986).
30. P. D. THOMAS, V. J. BASUS, AND T. L. JAMES, *Proc. Natl. Acad. Sci. USA* **88,** 1237 (1991).
31. D. A. BASSOLINO, F. HIRATA, D. B. KITCHEN, D. KOMINOS, A. PARDI, AND R. M. LEVY, *Int. J. Supercomput. Appl.* **2,** 41 (1988).
32. R. M. LEVY, D. A. BASSOLINO, AND D. B. KITCHEN, *Biochemistry* **28,** 9361 (1989).
33. D. B. KITCHEN, F. HIRATA, J. D. WESTBROOK, R. LEVY, D. KOFKE, AND M. YARMUSH, *J. Comp. Chem.* **11,** 1169 (1990).
34. W. A. HENDRICKSON AND M. M. TEETER, *Nature* **290,** 107 (1981).
35. A. ABRAGAM, "The Principles of Nuclear Magnetism," Oxford Univ. Press, Oxford, 1978.
36. S. J. WEINER, P. A. KOLLMAN, D. T. NGUYEN, AND D. A. CASE, *J. Comp. Chem.* **7,** 230 (1986).
37. W. J. METZLER, D. R. HARE, AND A. PARDI, *Biochemistry* **28,** 7045 (1989).
38. A. GRONENBORN AND G. M. CLORE, *Biochemistry* **28,** 5978 (1989).